Response of ENSO and the Mean State of the Tropical Pacific to Extratropical Cooling and Warming: A Study Using the IAP Coupled Model

Y. YU

LASG, Institute of Atmospheric Physics, Beijing, China

D.-Z. SUN

University of Colorado, CIRES Climate Diagnostics Center, NOAA/Earth System Research Laboratory, Boulder, Colorado, and School of Human Settlement and Civil Engineering, Xian Jiaotung University, Xian, China

(Manuscript received 24 October 2008, in final form 3 June 2009)

ABSTRACT

The coupled model of the Institute of Atmospheric Physics (IAP) is used to investigate the effects of extratropical cooling and warming on the tropical Pacific climate. The IAP coupled model is a fully coupled GCM without any flux correction. The model has been used in many aspects of climate modeling, including the Intergovernmental Panel on Climate Change (IPCC) Fourth Assessment Report (AR4) climate change and paleoclimate simulations. In this study, the IAP coupled model is subjected to cooling or heating over the extratropical Pacific. As in an earlier study, the cooling and heating is imposed over the extratropical region poleward of 10°N–10°S.

Consistent with earlier findings, an elevated (reduced) level of ENSO activity in response to an increase (decrease) in the cooling over the extratropical region is found. The changes in the time-mean structure of the equatorial upper ocean are also found to be very different between the case in which ocean–atmosphere is coupled over the equatorial region and the case in which the ocean–atmosphere over the equatorial region is decoupled. For example, in the uncoupled run, the thermocline water across the entire equatorial Pacific is cooled in response to an increase in the extratropical cooling. In the corresponding coupled run, the changes in the equatorial upper-ocean temperature in the extratropical cooling resemble a La Niña situation—a deeper thermocline in the western and central Pacific accompanied by a shallower thermocline in the eastern Pacific. Conversely, with coupling, the response of the equatorial upper ocean to extratropical cooling resembles an El Niño situation. These results ascertain the role of extratropical ocean in determining the amplitude of ENSO. The results also underscore the importance of ocean–atmosphere coupling in the interaction between the tropical Pacific and the extratropical Pacific.

1. Introduction

El Niño–Southern Oscillation (ENSO) is a prominent mode of the climate system and affects climate worldwide (Trenberth et al. 1998). Understanding the fundamental forces that control the level of ENSO activity is a basic issue in the study of climate dynamics. While our understanding of many aspects of ENSO is quite advanced (Neelin et al. 1998), the understanding of global factors controlling the level of ENSO activity is still limited (Wang and Picaut 2004; Sun 2004).

Among the global factors that have been suggested to be potentially important in influencing ENSO are the subtropical–extratropical cooling or heating. Using a coupled model, Bush and Philander (1998) investigated the impact of extratropical cooling associated with the Last Glacial Maximum on the tropical Pacific SST. They found that the tropical air–sea interaction amplifies the cooling effect from the high latitudes on the tropics. The attributed this amplification to two factors: 1) the positive Bjerknes feedback within the tropics (Neelin et al. 1998) and 2) the exchange of water between the tropics and extratropics through the ''ocean tunnel''—surface water of the extratropical ocean is subducted downward and equatorward to feed the equatorial undercurrent and therefore the equatorial upwelling (Pedlosky 1987; Liu et al. 1994; McCreary and

Corresponding author address: Yongqiang Yu, LASG, Institute of Atmospheric Physics, Beijing 100029, China.
E-mail: yyq@lasg.iap.ac.cn

DOI: 10.1175/2009JCLI2902.1

Lu 1994). They did not analyze, however, the corresponding changes in ENSO amplitude. Using a simple box model, Sun (1997, 2000) suggested that the amplitude of ENSO may depend on the subsurface temperatures and therefore raised the possibility that extratropical–subtropical cooling and warming may influence the amplitude of ENSO as the equatorial thermocline water comes from the extratropical–subtropical ocean. Using a hybrid coupled model—the National Center for Atmospheric Research (NCAR) Pacific basin model coupled to an empirical atmosphere—Sun et al. (2004) conducted numerical experiments to further investigate the response of the ENSO amplitude to imposed extratropical cooling and warming. They found that the level of ENSO activity increases in response to an increase in the extratropical cooling. They explain this result by noting that the extratropical cooling eventually cools the equatorial thermocline water and thereby destabilizes the coupled equatorial ocean–atmosphere system. The stronger ENSO is a response to this destabilizing forcing. Conversely, they found that an extratropical warming (or a decrease in extratropical cooling) reduces the level of ENSO activity. Combined with the results from an earlier study on the impact of an increase in the radiative heating over the tropics on the ENSO amplitude (Sun 2003), the results of Sun et al. (2004) link the amplitude of ENSO to the meridional differential heating over the Pacific Ocean and thereby to the heat uptake of the tropical Pacific and poleward heat transport from that region. Fedorov et al. (2006) also suggested an important role of extratropical warming and cooling and the poleward heat transport in determining the level of ENSO activity. In particular, they suggested that the apparent lack of ENSO activity 3 million years ago may be a consequence of a much warmer extratropics during that period (Fedorov et al. 2006). In the same vein, they suggest that the subsequent onset of ENSO was a response to the gradual cooling in the extratropics taking place since 3 million years ago.

Following upon the study of Sun et al. (2004), Sun and Zhang (2006) further showed that the response of the time-mean state of the tropical Pacific to extratropical cooling is very different in the case when the equatorial ocean–atmosphere is coupled (the case with ENSO) and in the case when the equatorial ocean–atmosphere is not coupled. Their results suggest that ENSO has a time-mean effect on the time-mean state. [Specifically, the study of Sun and Zhang (2006) suggests that ENSO events, collectively, may act as a basin-scale heat mixer that prevents the time-mean difference between the warm pool SST and the temperature of the equatorial thermocline water from exceeding a critical value.] As suggested by Rodgers et al. (2004), Schopf and Burgman (2006), and Sun and Yu (2009), ascertaining and understanding the time-mean effect of ENSO could be critical to a better understanding of the decadal variability in the tropical Pacific.

The twin questions addressed by aforementioned studies—what is the role of extratropical cooling in determining the amplitude of ENSO and what is the feedback from ENSO on the mean climate of the tropical Pacific—are obviously important for understanding factors outside the tropical Pacific in determining the level of ENSO activity and more generally for understanding the role of ocean–atmosphere interaction in tropical–extratropical communication in the climate system. The present investigation aims to further address these questions. The focus is on understanding, so we take a step-by-step approach by following the methodology used in Sun et al. (2004) closely. We will, however, use a more sophisticated coupled model—both components of the model are GCMs. The paper is organized as follows: The model and experiment design is discussed in section 2. In section 3, we present the main results. Summary and discussion are provided in section 4.

2. Model description and experiment design

The gridpoint version 1.1 (g1.1) of the Institute of Atmospheric Physics (IAP) coupled GCM Flexible Global Ocean–Atmosphere–Land System Model (FGOALS) is used in this study to investigate the effect of the extratropical cooling and warming on ENSO behavior. The coupled GCM consists of four interactive components: atmospheric, oceanic, land, and sea ice models connected by NCAR flux coupler version 5 (Collins et al. 2003). The oceanic component model is a State Key Laboratory of Numerical Modeling for Atmospheric Sciences and Geophysical Fluid Dynamics (LASG)/IAP Climate system Ocean Model (LICOM) version 1.1 (Zhang et al. 2003; Liu et al. 2004; Xiao and Yu 2006). In this study, the horizontal resolution of LICOM was subscribed to $1.0° \times 1.0°$, and 30 levels are used in vertical with 12 equal levels in the upper 300 m. The atmospheric component model is a gridpoint model: the Atmospheric Model of IAP/LASG (GAMIL). The dynamical core includes a finite-difference scheme that conserves total mass and energy in solving the primitive hydrostatic equations of a baroclinic atmosphere (Wang et al. 2004), and a two-step shape-preserving advection scheme for the moisture equation (Yu 1994). The model employs a hybrid horizontal grid with a Gaussian grid of 2.8° between 65.58°S and 65.58°N and weighted equal-area grid poleward of 65.58°. There are 26 σ layers from the surface to 2.19 hPa. The physics package was taken

from the NCAR Community Atmospheric Model version 2 (CAM2) (Collins et al. 2003). The sea ice and land component models are, respectively, the NCAR Sea Ice Model (CSIM4) (Bettge et al. 1996) and the NCAR Common Land Model (CLM2.0) (Bonan et al. 2002). We adjust the land–sea mask and horizontal resolution of land and sea ice models to match those of atmospheric and oceanic models. More details of the model can be found in Yu et al. (2008).

In this study, in order to be consistent with the way cooling and warming are applied in Sun et al. (2004), we stripped the full FGOALS to a simpler version in which daily heat, momentum, and freshwater fluxes are exchanged in the tropical Pacific between 10°S and 10°N only. Outside of 10°S–10°N in the tropical Pacific, the AGCM and OGCM are not coupled but forced with the observed forcing. The AGCM is forced with the observed climatological SST and sea ice distribution. The OGCM is forced with the observed climatological wind stress, freshwater flux, and heat flux calculated from

TABLE 1. A summary of the experiments.

Experiment	Coupling	Extratropical conditions	ENSO?
A	10°S–10°N	Climatology	Yes
B	10°S–10°N	Warming	Yes
C	10°S–10°N	Cooling	Yes
D	None	Climatology	No
E	None	Warming	No
F	None	Cooling	No

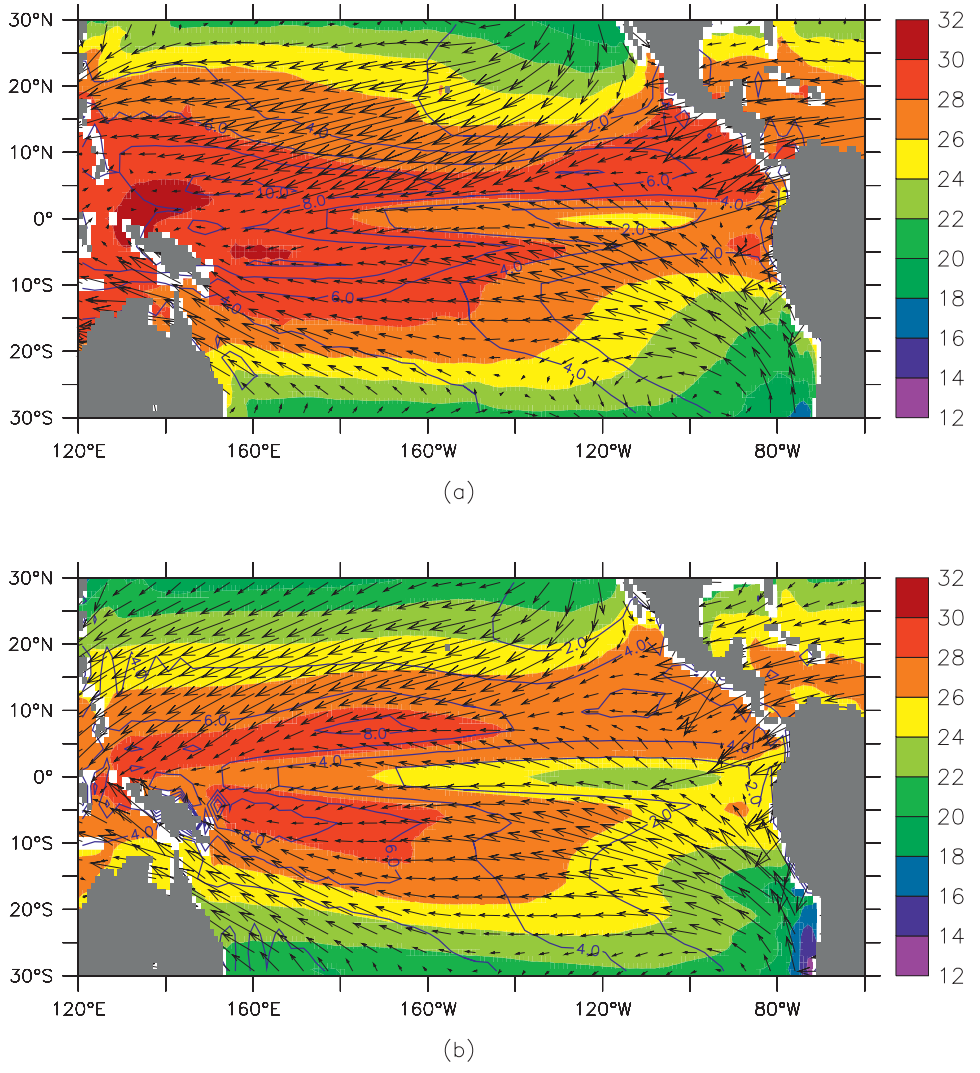

FIG. 1. Climatological annual mean SST (shaded, °C), precipitation (contours, mm day^{-1}), and wind stress (vectors, N m^{-2}) in the tropical Pacific from the control run by the (a) tropically coupled GCM and (b) globally coupled GCM. (Data from the 41st to 80th model year were used.)

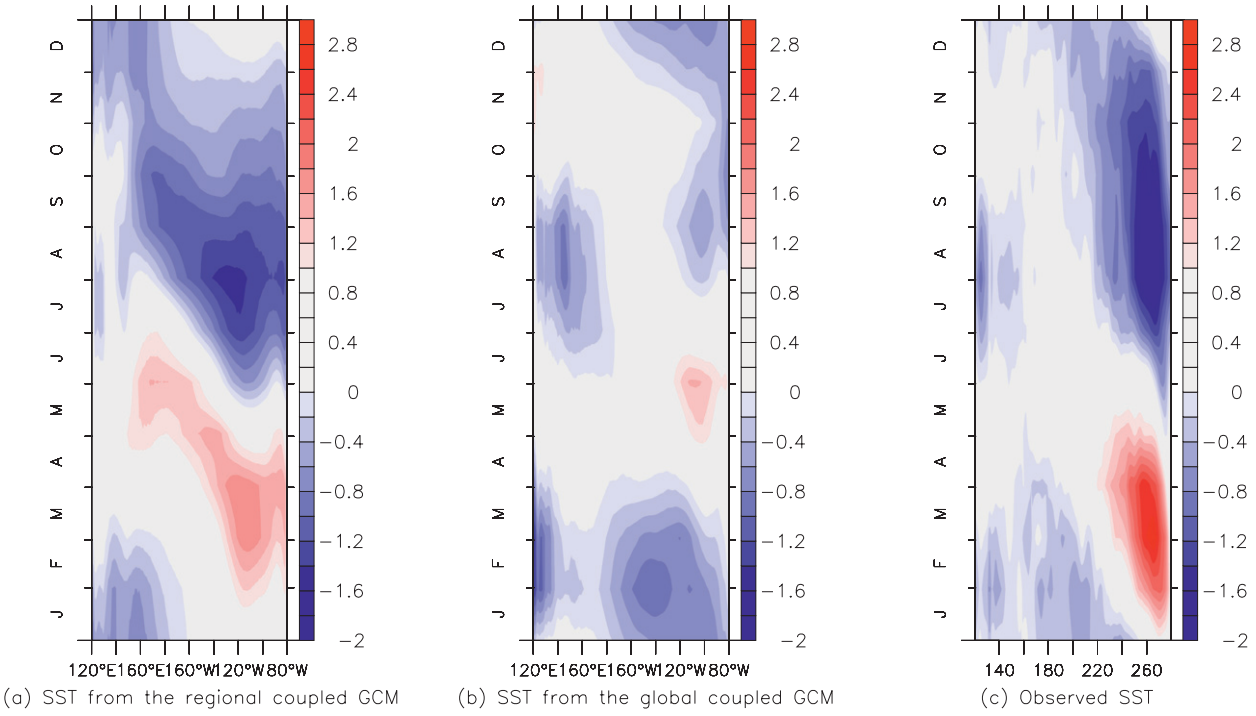

FIG. 2. The seasonal cycle of the SST (averaged over 2°S–2°N) for the two versions of the model and the observations—(a) the tropically coupled only version and (b) the globally coupled version—and (c) the observations.

a restoring thermal boundary condition in which the restoring SST is the observed climatological SST. We conducted a control run, an extratropical cooling run, and an extratropical warming run with this coupled GCM. The extratropical cooling and warming imposed over the ocean's surface are the same as in Sun et al. (2004). The length of the run for all three runs is 80 yr. We use the last 40 model years in this study.

To isolate the effects of the air–sea interaction on the response of the mean tropical Pacific climate to extratropical warming and cooling, we carry out three additional experiments with the ocean component model of the aforementioned coupled GCM: a control run, an extratropical cooling run, and an extratropical warming run. The perturbations are again either extratropical cooling or warming and take the same form as in the coupled experiments. For these three uncoupled experiments with the ocean component, we use climatological surface forcing everywhere including the equatorial region (i.e., the wind stress, the restoring SST, and

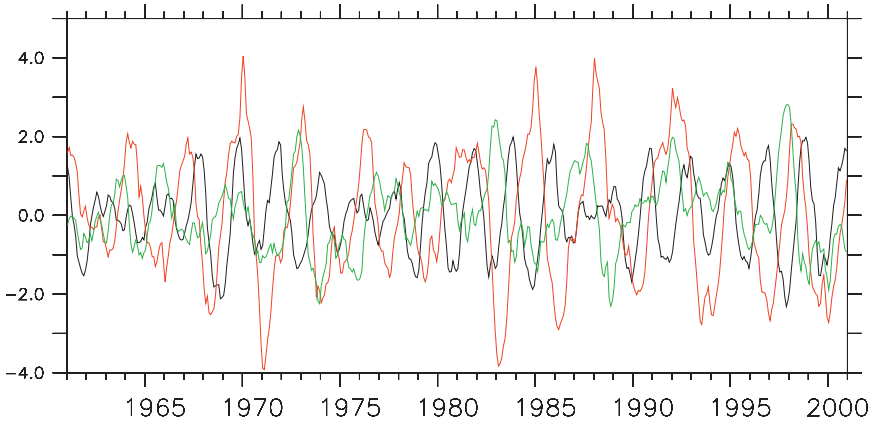

FIG. 3. Monthly mean Niño-3.4 index from the control run of the tropically coupled GCM (red) and the full version (black) and observation (green) (°C).

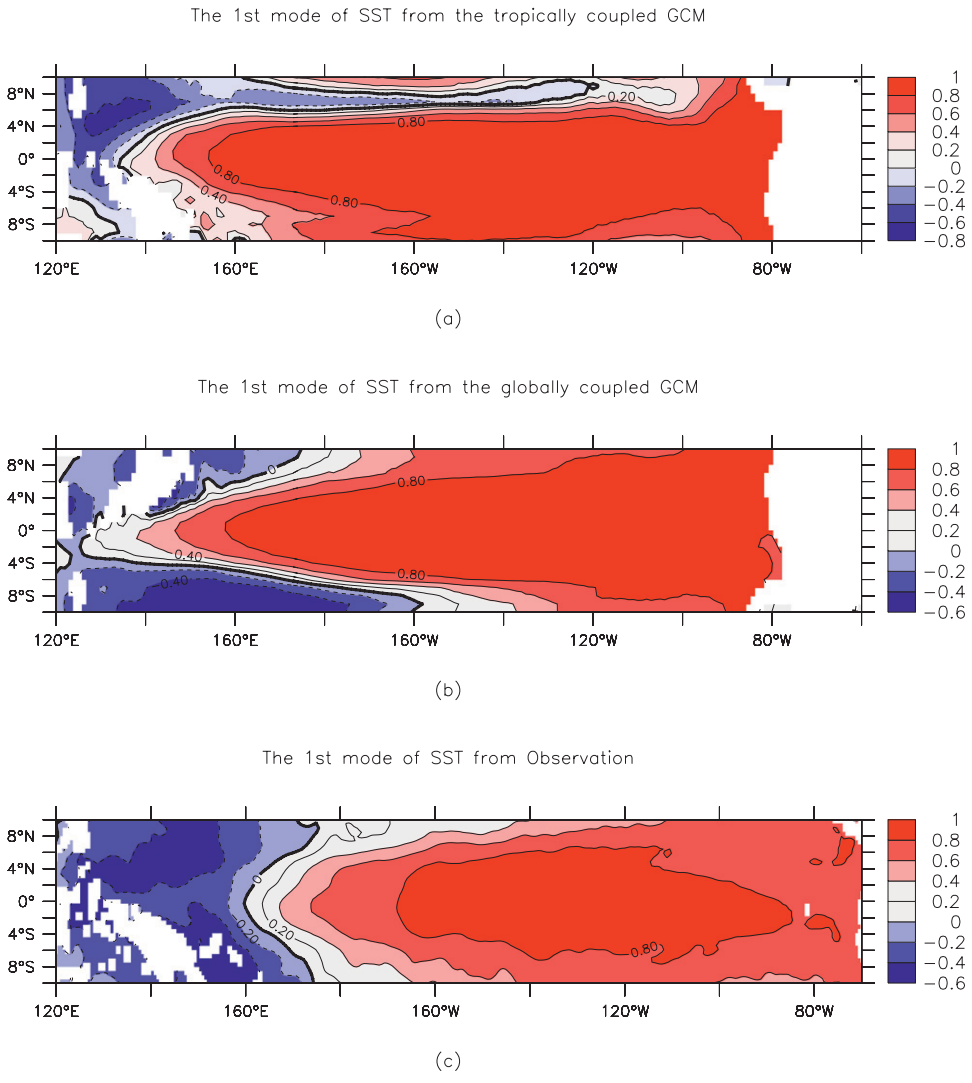

FIG. 4. Spatial pattern of SST anomaly associated with ENSO as represented by the leading EOF of the tropical Pacific SST variability within the region 10°S–10°N for (a),(b) the control run of the two versions of the model and (c) the observations. Recall that the coupling is restricted to the equatorial region (10°S–10°N).

freshwater flux that have no interannual variations). Thus, in these experiments, there are no ENSO events.

Thus, as in Sun et al. (2004), for either extratropical cooling or warming, we have a pair of experiments—one of the experiments is coupled over the equatorial region (we call this experiment the case with ENSO or simply the coupled run) and the other experiment is not coupled (we call this experiment the case without ENSO or simply the uncoupled run). The coupled runs are 80 yr long—the last 40 yr were used in the analysis. The forced experiments are 50 yr long and the last 10 yr were used for the analysis. Note that the purpose here is not to compare which run is closer to the observations, but to examine the influence of equatorial ocean–atmosphere coupling on the response of the tropical Pacific climate to an imposed extratropical forcing. A summary of the experiments is given in Table 1.

3. Results

a. Control run

Figure 1 shows the climatological annual mean SST (color), precipitation (contour), and wind stress (arrows) of the control run in the tropical Pacific from the tropically coupled GCM (coupling is restricted to the tropical Pacific) and from the full version (globally coupled). The change in the large-scale pattern of SST, wind stress, and precipitation from the full version to the

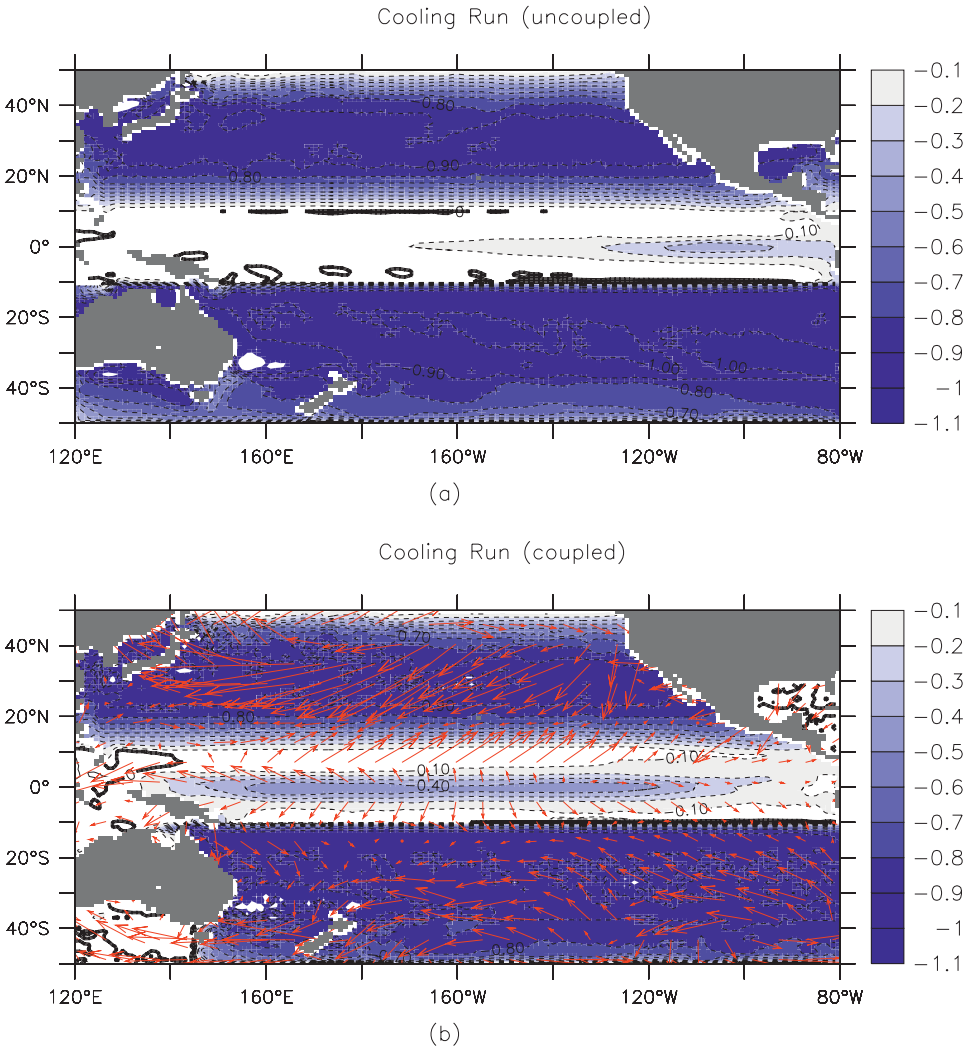

FIG. 5. (a) SST differences between the uncoupled extratropical cooling run and the control run. (b) SST differences between the coupled extratropical cooling run and the control run (°C). The corresponding differences in the surface wind stress are shown as arrows (N m^{-2}). For the coupled run, the 41st to 80th model years were used in the calculation. For the uncoupled run, the last 10 yr of a 50-yr-long forced run were used.

stripped-down version is small. In comparison with observations, there remains a cold bias in the central equatorial Pacific and a warm bias in the southeastern Pacific. The cold and warm SST biases are accompanied by overestimated and underestimated rainfall biases, respectively, over these two regions. Consequently, the simulated precipitation appears to be more symmetric about the equator than in the observations, exhibiting the so-called double ITCZ syndrome (Mechoso et al. 1995)—a common bias in the state-of-art coupled models that do not use flux adjustment (Sun et al. 2006). The tropically coupled model has a slightly warmer cold tongue than the full version. The annual cycle in the stripped-down version is notably more realistic than in the full version (Fig. 2). Both versions have pronounced interannual variability. Figure 3 shows the time series of the Niño-3.4 SST anomaly from the tropically coupled model together with the corresponding time series from the full model. The observed Niño-3.4 SSTs over the last 40 yr are also shown for comparison. The amplitude of ENSO in the tropically coupled model is weaker than in the full version but more comparable to the observed. The period of the ENSO in the tropically coupled model is more biannual than the full version. ENSO in both versions is more regular and stronger than in the observations. These differences from observations are common in coupled GCMs (van Oldenborgh et al. 2005). The spatial patterns of the SST anomaly–associated ENSO

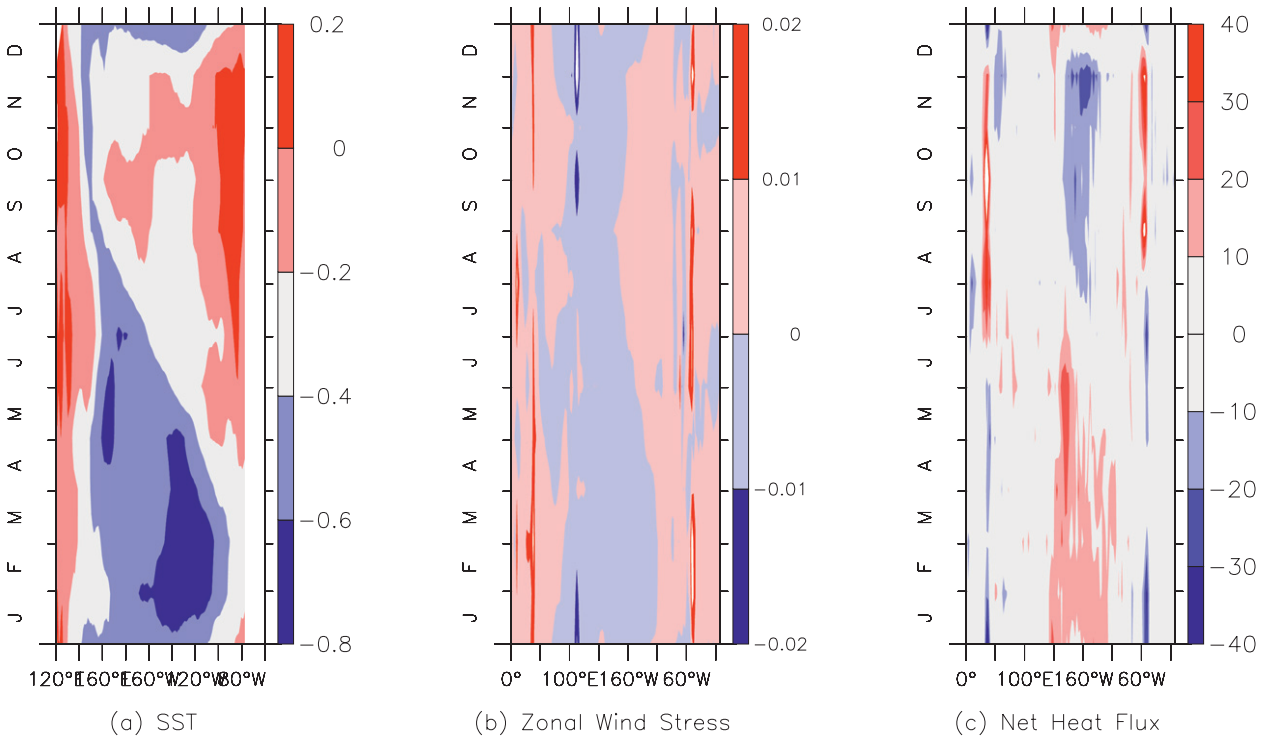

FIG. 6. (a) The seasonal march of the SST differences between the coupled extratropical cooling run and the control run (°C). The corresponding seasonal march of the (b) zonal wind stress differences (N m^{-2}) and (c) net surface heat flux differences (W m^{-2}).

from these two versions and the observations are shown in Fig. 4. As in many other coupled models, the anomaly extended too far to the west, but the overall feature resembles the observations well. More detailed discussion about the climatology and variability in this model can be found in (Yu et al. 2008).

b. Extratropical cooling experiments

Figures 5a and 5b show, respectively, the response of the climatological annual mean SST in the case without ENSO (equatorial ocean–atmosphere is not coupled) and in the case with ENSO (equatorial ocean–atmosphere is coupled) to the extratropical cooling. In the uncoupled experiment (Fig. 5a), the response of the SST of the equatorial Pacific to the imposed cooling about 1°C over the extratropical Pacific is weak: the cooling is less than 0.2°C and is confined to the eastern Pacific only. When air–sea interaction is considered in the coupled model, however, the cooling to the equatorial surface ocean is enhanced to about 0.4°C, and this cooling extends to the western tropical Pacific (Fig. 5b). The corresponding seasonal march of the SST difference between the extratropical cooling and control runs from the coupled GCM is further shown in Fig. 6a together with the corresponding seasonal march of the zonal wind stress and the net surface heat flux. The figure shows a reduced seasonal cycle. The strongest cooling is about 0.8°C and occurs in the first half year (Fig. 6a), and this corresponds to a period with enhanced easterly wind stress in the middle and western Pacific (Fig. 6b). The corresponding evolution of the changes in the net surface heat flux shows that it acts as a negative feedback that damps the SST changes (Fig. 6c).

The response of the entire equatorial upper-ocean temperature to the imposed extratropical cooling is shown in Fig. 7. The upper panel is for the case without ENSO (uncoupled run), and the bottom one is for the case with ENSO (coupled run). In the case without ENSO, the maximum cooling can be found in the thermocline with maximum value about 0.7°C. As in the experiments of Sun et al. (2004), the cooling is largely confined to the subsurface. The surface cooling is only 0.2°C. Note that the sea surface temperature is restored to the observed SST in the uncoupled model. The cooling to the surface is largely limited to the eastern Pacific, resulting in a weak increase in the zonal SST contrast.

In the coupled run, the response of the equatorial upper-ocean temperature has an almost completely different pattern: the subsurface cooling is substantially reduced. In fact, the subsurface of the western Pacific even has slightly positive anomaly. The cooling is no longer confined to the subsurface ocean. Instead, it

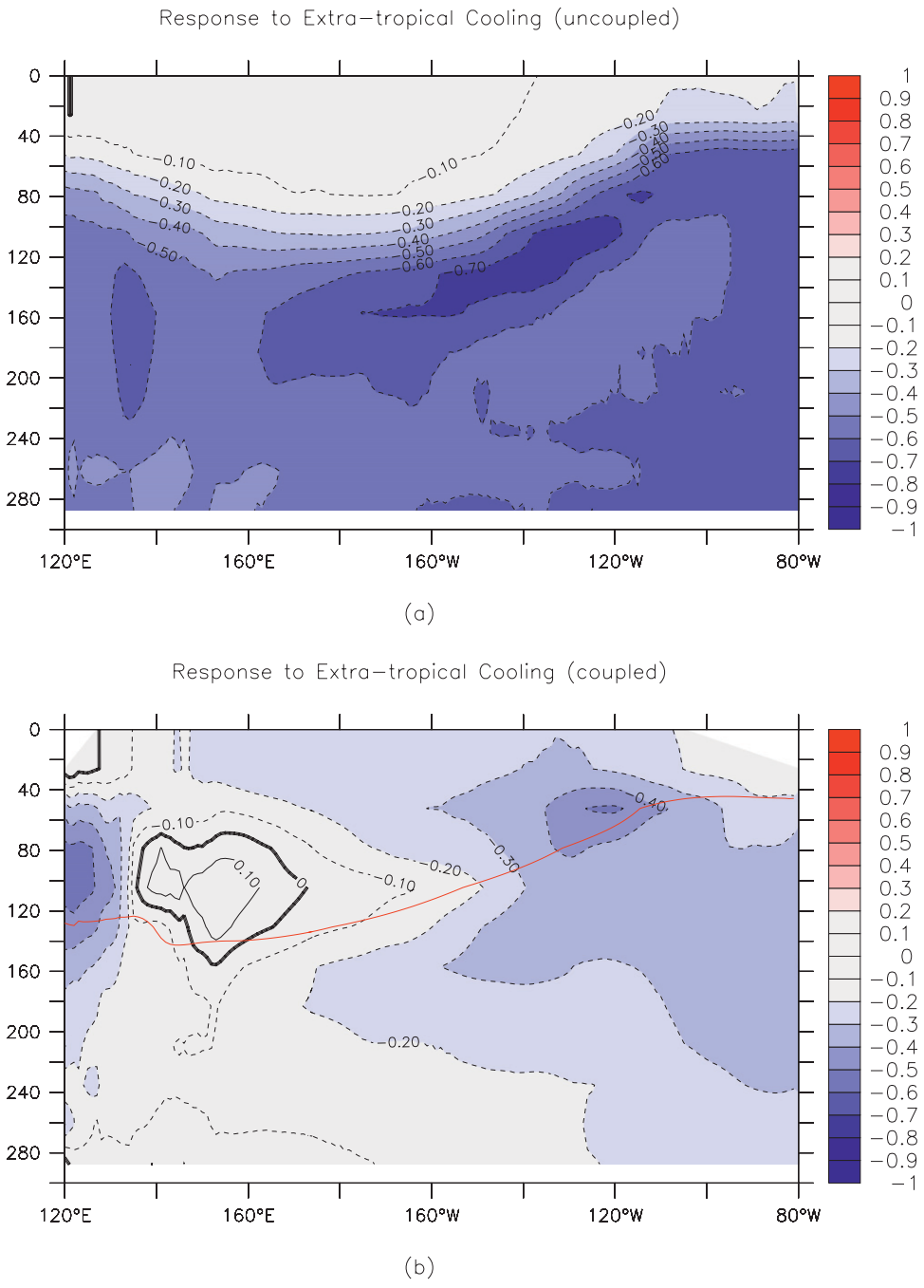

FIG. 7. Depth–longitude section of temperature difference (°C) along the equator (a) between the extratropical cooling run without ENSO and the control run and (b) between the extratropical cooling run with ENSO and the control run. The red line indicates the position the 20°C isotherm in the control run. The data used are the same as for Fig. 5.

extends to the surface of the entire equatorial ocean. Because in this case the equatorial zonal wind stress is coupled to the SST gradients, the subsurface temperature is not only affected by the extratropical cooling but also by the zonal wind stress in the coupled run. Because the extratropical cooling to the equatorial upwelling water through the ''ocean tunnel'' (Pedlosky 1987; Liu et al. 1994; McCreary and Lu 1994) alone results in an increased zonal SST contrast (Fig. 7a), the zonal wind stress is then enhanced. The enhanced zonal wind stress

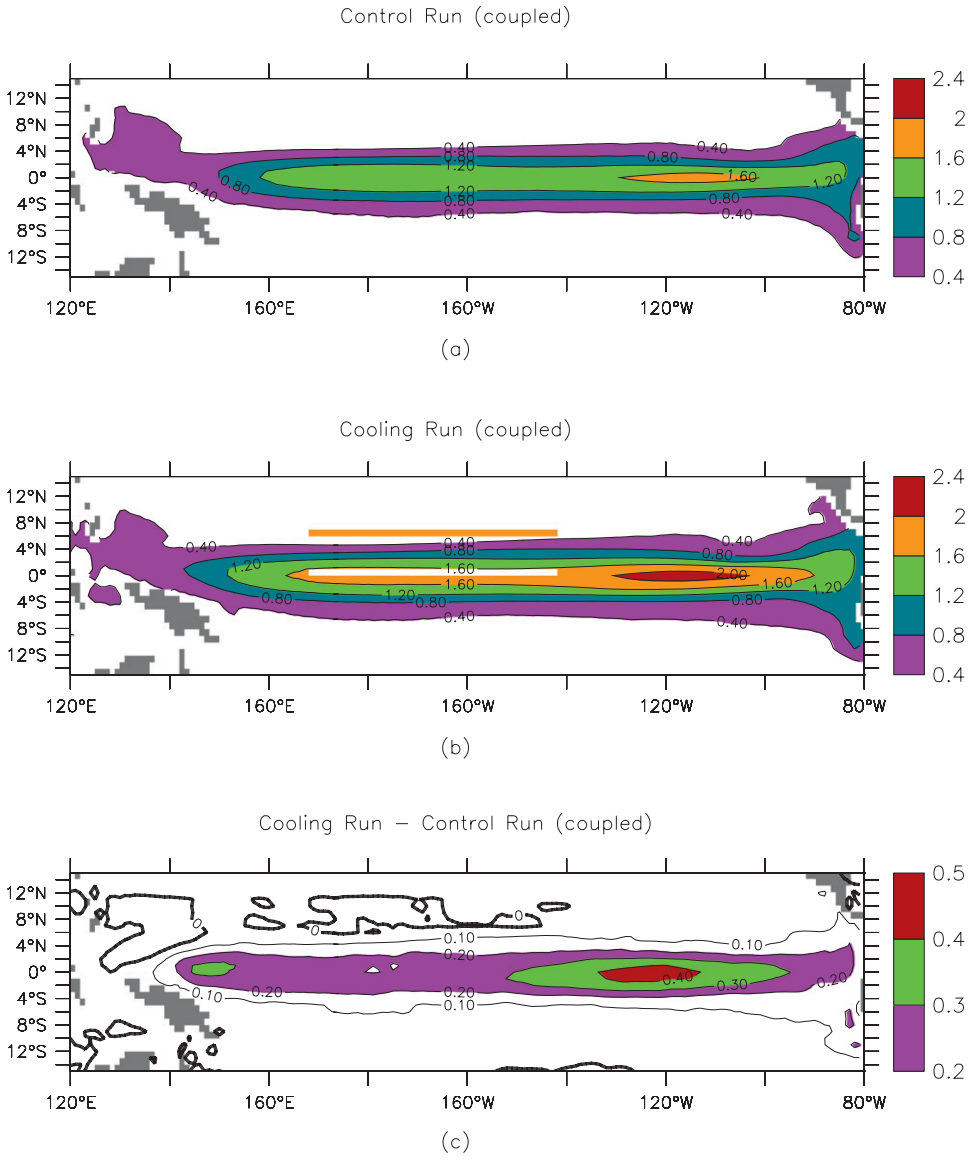

FIG. 8. Standard deviation of monthly mean sea surface temperature for (a) the control run, (b) the extratropical cooling run, and (c) the difference between the two runs (°C). Note that both runs are coupled runs. The data used are the same as for Fig. 5.

can deepen mean depth as well as the zonal tilt of thermocline (Jin 1996; Sun 1997)—a configuration that favors stronger ENSO events. Figure 8 shows the standard deviation of monthly mean SST from the control and extratropical cooling runs by the coupled GCM. The ENSO amplitude is enhanced in the extratropical cooling run. As shown in Fig. 7a, in the absence of coupling, the imposed extratropical cooling increases the temperature contrast between the western Pacific surface water and the thermocline water and thereby constitutes a destabilized effect of the ocean–atmosphere system. A stronger ENSO is expected to neutralize this destabilization.

The meridional section of temperature changes averaged between 90° and 150°W from the extratropical cooling run is shown in Fig. 9. Although the external forcing is superimposed in the extratropical surface ocean, both coupled and uncoupled runs show a relatively large surface cooling centered at the equator. The weakest surface cooling can be found between 5° and 10°N(S). This pattern of cooling is consistent with the ''ocean tunnel'' effect: colder water penetrates into the equatorial thermocline through subduction along isentropic surfaces (Pedlosky 1987; Liu et al. 1994; McCreary and Lu 1994). Consequently, the surface water off the equator

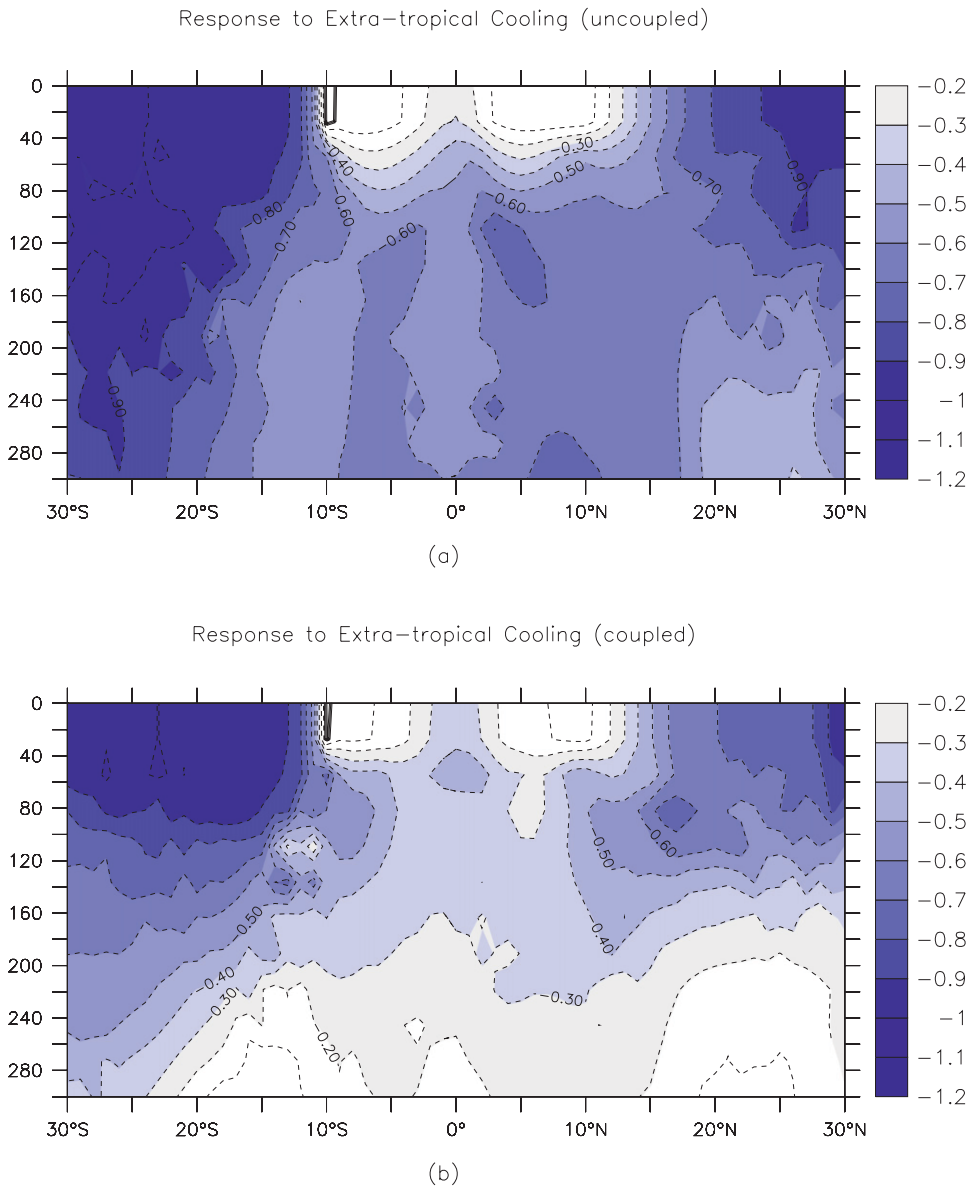

FIG. 9. Depth–latitude section of temperature difference (°C) (a) between extratropical cooling run without ENSO and the control run and (b) between the extratropical cooling run with ENSO and the control run. The data used are the same as for Fig. 5.

between 5° and 10°N(S) is hardly affected by the extratropical cooling. Having compared temperature changes from the uncoupled run with those from coupled run, two distinctive things can be found. The first one is that the subsurface cooling along the equator is weakened in the coupled run, as shown in Fig. 7. This is due to stronger vertical water exchange in the coupled run induced by air–sea interaction. On the other hand, the amplitude of cooling in the extratropical region in both the surface and subsurface is also reduced in the coupled run. Because the air–sea interaction is turned off in the extratropical region and the same external forcing is applied in coupled and uncoupled runs, the weakened extratropical cooling in the coupled run results from an enhanced poleward heat transport by oceanic circulation.

c. *Extratropical warming experiments*

Extratropical warming experiments generally show reversed patterns from the extratropical cooling ones. Figure 10 shows the SST changes in response to an imposed extratropical warming. The upper panel is for the case without ENSO (uncoupled run) and the lower

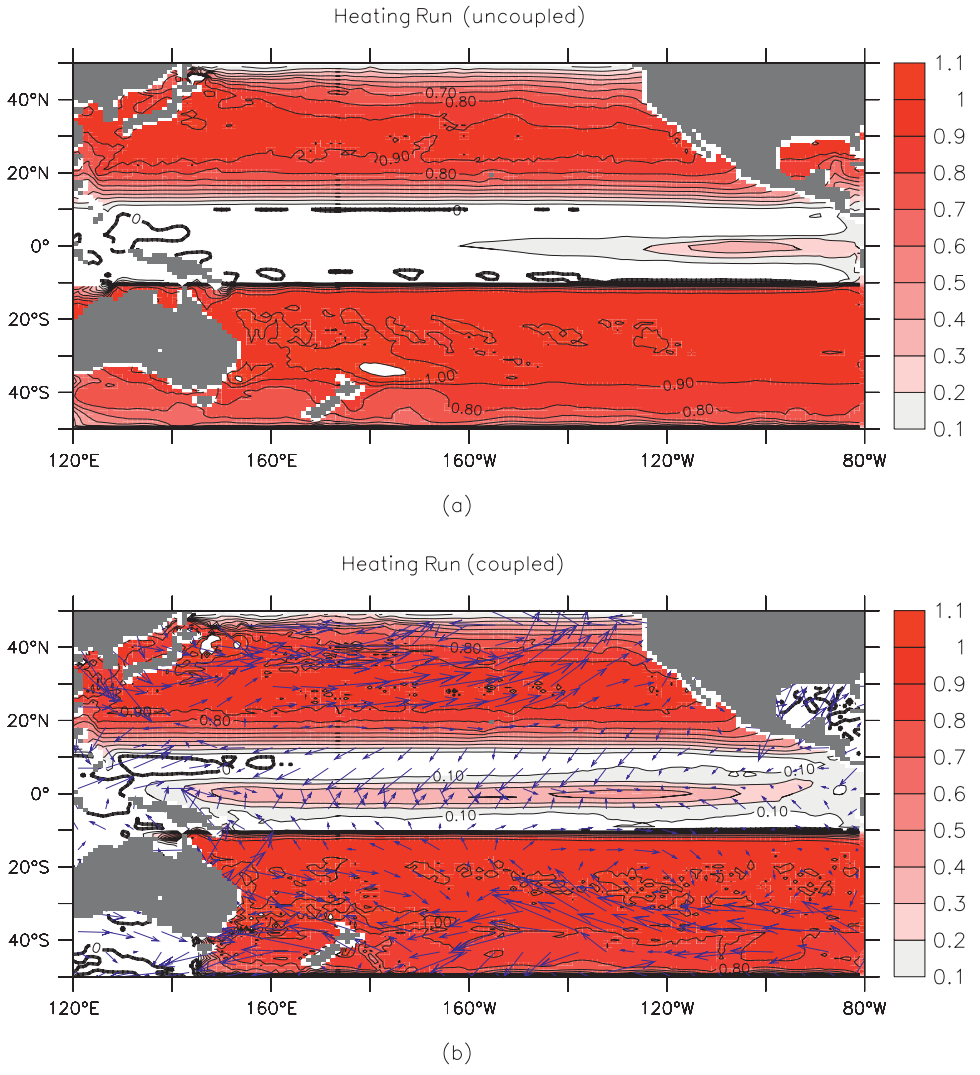

FIG. 10. (a) SST differences between the uncoupled extratropical warming run and the control run. (b) SST differences between the coupled extratropical warming run and the control run (°C). The corresponding differences in the surface wind stress are shown as arrows (unit: N m^{-2}). For the coupled run, the 41st to 80th model year were used in the calculation. For the uncoupled run, the last 10 yr of a 50-yr-long forced run was used.

panel is for the case with ENSO (coupled run). In the case with ENSO, the extratropical warming leads to about 0.2°C warming in the eastern equatorial Pacific (Fig. 10b). In the case with ENSO, the tropical warming is strengthened to 0.4°C and the warming extends all the way to the western Pacific.

Figure 11 shows equatorial temperature changes from extratropical warming experiments in the case without ENSO and the case with ENSO. Figure 11a is for the case without ENSO, and Fig. 11b is for the case with ENSO. Figures 11a,b are about the reverses of Figs. 7a,b. In the absence of coupling, the effect of the imposed extratropical warming on the equatorial upper-ocean temperature is largely confined to the thermocline. In the presence of coupling, the response of the upper-ocean temperature resembles an El Niño pattern. The eastern Pacific is much warmer while the subsurface of the western Pacific actually gets cooler.

Closer comparison between the warming case and the cooling case reveals differences that may be of significance. The imposed cooling and the heating over the extratropical Pacific is the same, but Figs. 7a and 11a show that the equatorial thermocline temperature response to the cooling more sensitively (0.7°C cooling versus 0.5°C warming). There are no noticeable asymmetries in the coupled experiments, though. In response to the

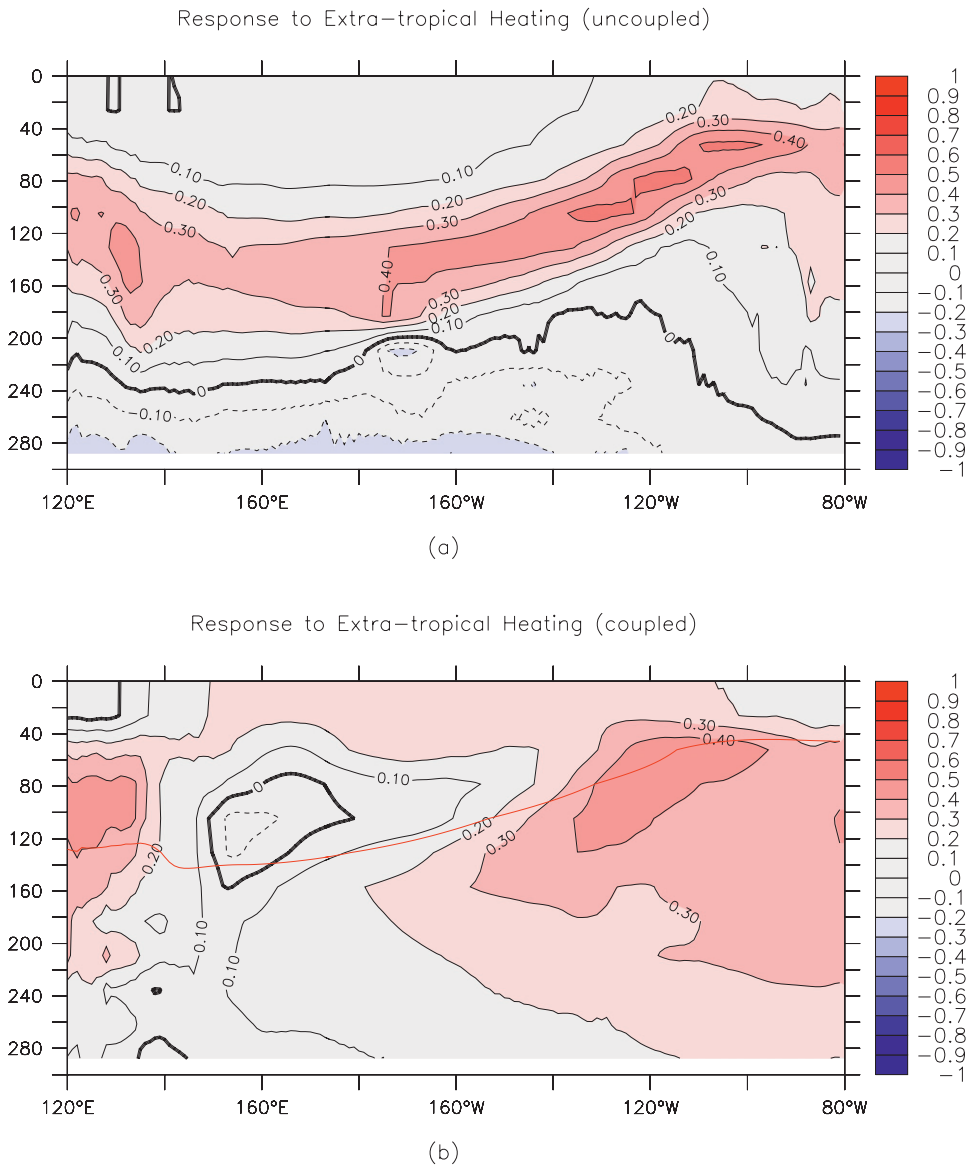

FIG. 11. Depth–longitude section of temperature difference (°C) along the equator (a) between the extratropical warming run without coupling and the control run and (b) between the extratropical warming run with coupling and the control run. The data used are the same as for Fig. 10.

weakened zonal SST gradients, the zonal winds become weaker, which results in a flattening and shoaling of the thermocline. Compared with the control run of coupled model, the extratropical warming run reveals pronounced subsurface warming along the thermocline, consequently resulting in a weakened temperature contrast between surface temperature in the western Pacific and that in the thermocline. This change implies a stabilized effect of the ocean–atmosphere system. Indeed, in the case with warming imposed, ENSO is weaker (Fig. 12).

The pattern of the meridional section of temperature changes from extratropical warming is quite similar to the case of extratropical cooling, but there are some differences (Fig. 13). For example, a uniform cooling can be found along the equator in the extratropical cooling case without ENSO, but in the corresponding extratropical warming case, the warming can only be found above 200 m. Below this depth in the extratropical warming case, the response is actually cooling. In the coupled case (i.e., the case with ENSO), the coupled extratropical cooling run shows weakened extratropical cooling in both hemispheres, and the coupled extratropical warming run shows weakened extratropical warming in the Southern Hemisphere only.

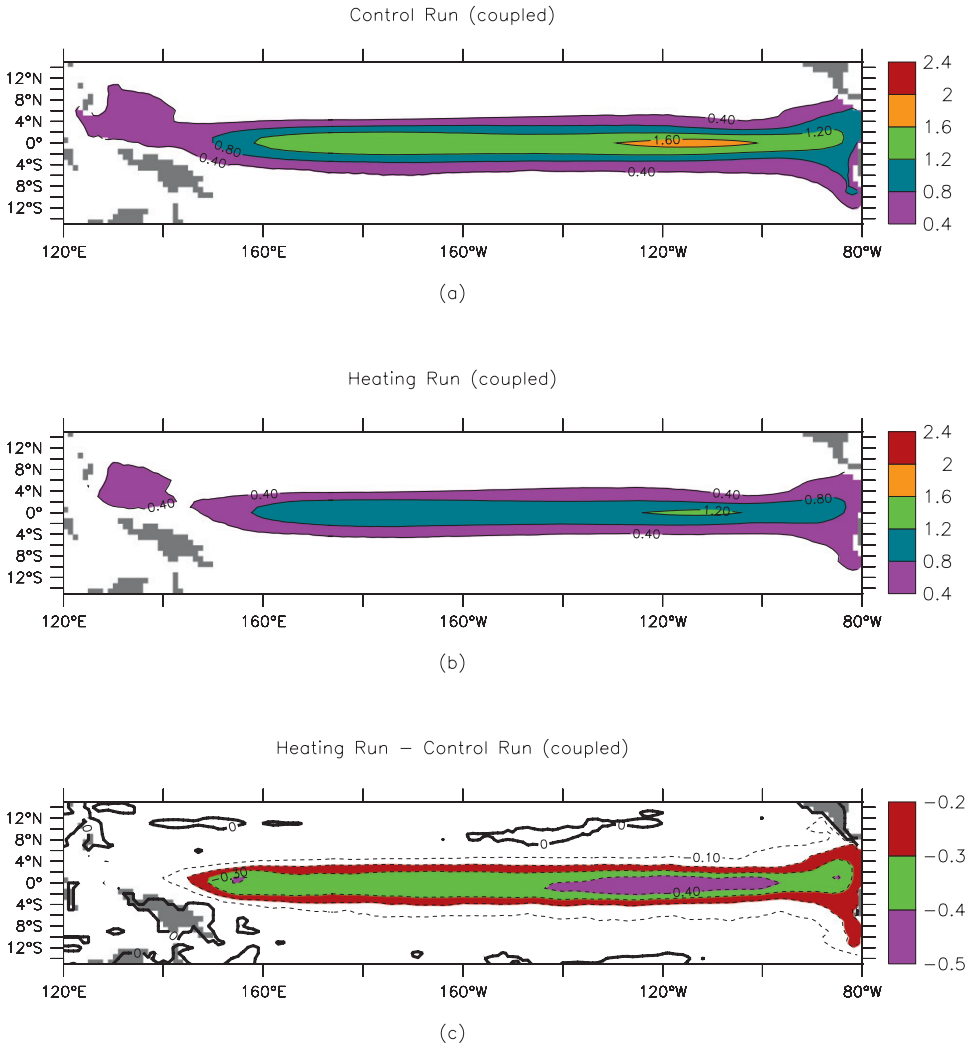

FIG. 12. Standard deviation of monthly mean sea surface temperature for (a) the control run, (b) the extratropical warming run, and (c) the differences between the two runs (°C). The data used are the same as for Fig. 10.

4. Summary

Following the study of Sun et al. (2004), we have conducted an extended investigation of the role of equatorial ocean–atmosphere coupling in extratropical and tropical interactions—particularly how the equatorial coupling affects the response of the tropical Pacific upper ocean to extratropical cooling and warming. The extratropical warming and cooling experiments are carried out with a regionally coupled GCM—ocean–atmosphere is only coupled over the equatorial Pacific. Experiments were conducted in pairs. In one of the experiments, ocean–atmosphere over the equatorial region is switched off, and therefore ENSO is not present. When the equatorial ocean–atmosphere is not coupled (no ENSO), extratropical cooling and warming respectively increases and decreases the thermal contrast between the warm pool SST (Tw) and the characteristic temperature of the equatorial thermocline water (Tc) (i.e., respectively destabilizes and stabilizes the coupled equatorial ocean–atmosphere system). Comparing coupled experiments with the uncoupled experiments, it can be found that the equatorial air–sea interaction (or the presence of ENSO) reduces the response of Tw–Tc through a stronger vertical exchange of heat induced by ENSO in the coupled run. ENSO amplitude is enhanced in the extratropical cooling run and reduced in the extratropical warming run. The response of ENSO amplitude to the cooling in the present model appears to be less sensitive, as in the model of Sun et al. (2004), possibly because the control run in the present model already has very strong ENSO. The response of ENSO

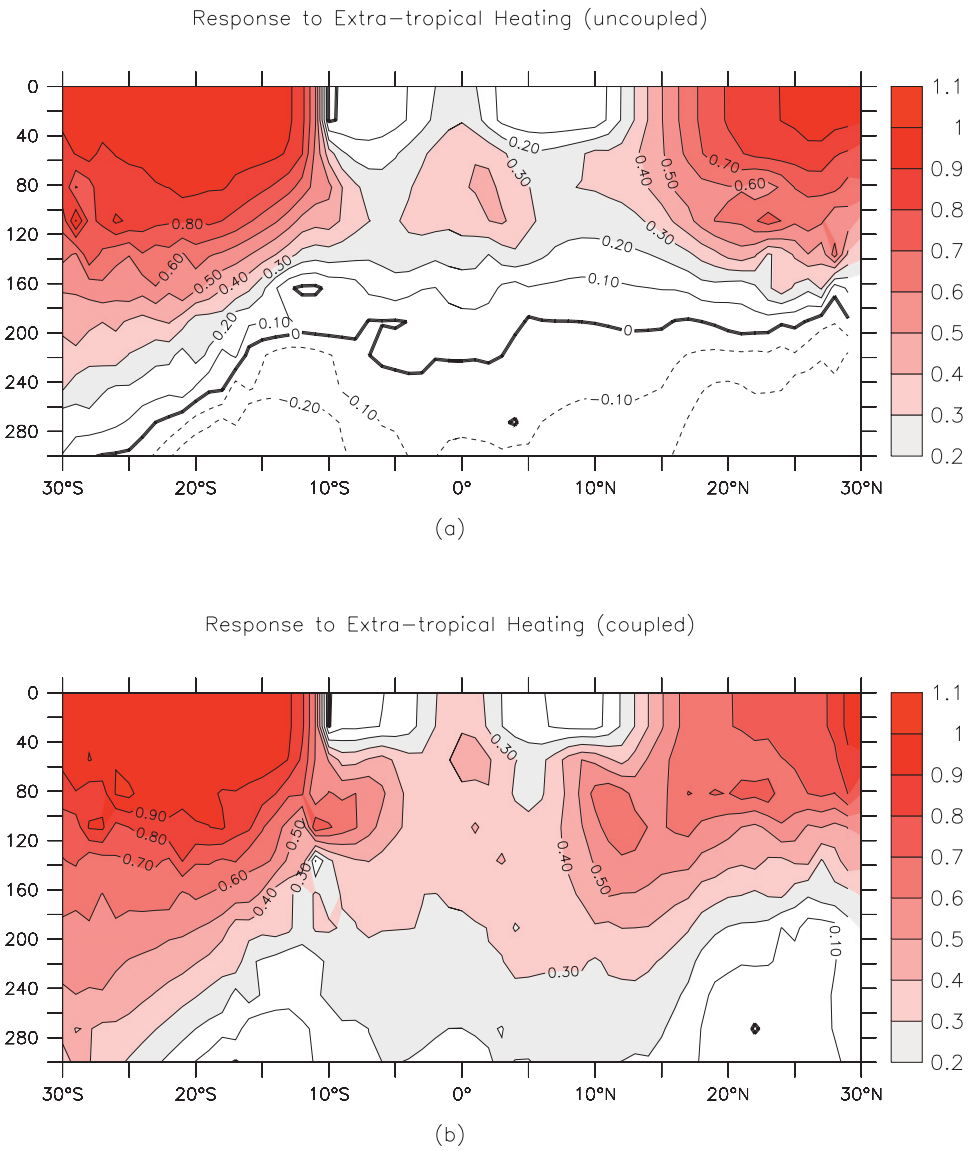

FIG. 13. Depth–latitude section of temperature difference (C) (a) between extratropical warming run without ENSO and the control run and (b) between the extratropical warming run with ENSO and the control run. The data used are the same as for Fig. 10.

frequency to extratropical cooling and heating is also compared, but we have not found any significant change in period. Also, by contrasting the extratropical warming runs with the corresponding cooling runs, we find that the mean tropical climate is more sensitive to extratropical cooling than to extratropical warming, particularly in the case in the absence of coupling, suggesting a potential role of the buoyancy effects.

To be in line with Sun et al. (2004), and taking a step-by-step approach, we have limited ocean–atmosphere coupling in the coupled experiments to the equatorial Pacific. We plan to carry out additional perturbation experiments in which the ocean and atmosphere over the extratropical Pacific are also allowed to couple. These experiments are more technically difficult but will allows us to investigate whether the role of ENSO as delineated in Sun et al. (2004) and in the present study in facilitating the remote forcing from the extratropical ocean onto the equatorial ocean still holds in a more realistic setting. As in other models, the present model has a cold bias. We will need to investigate whether and how the tropical cold bias may impact the response of the coupled model to extratropical cooling or warming.

Tropical–extratropical interaction though the ''ocean tunnel'' (Pedlosky 1987; Liu et al. 1994; McCreary and Lu 1994) has been hypothesized as an important

mechanism for decadal variability in the Pacific (Deser et al. 1996; Gu and Philander 1997). The role of ENSO—or more generally the equatorial ocean–atmosphere coupling—has not been adequately considered in these studies. By delineating the role of equatorial ocean–atmosphere coupling in the tropical–extratropical interaction, the present study may also help to advance our understanding of the decadal variability in the tropical Pacific. In the same vein, the present study may also help to understand the Pacific climate change over centennial and longer time scales. For example, Cobb et al. (2003) has found that during the Little Ice Age—a period during which significant cooling was registered in extratropical regions (Bradley et al. 2003), ENSO was more energetic than many other periods during the last millennium. Conversely, the proxy data by Rein et al. (2005) suggest a weak ENSO activity during the medieval warm period—a period during which significant warming was observed in the extratropical regions. The present study may help to understand these paleoclimate observations.

Because the climate response in the tropical Pacific to increased greenhouse gases has been paid more and more attention, the present study may also help to explain the response of the tropical Pacific climate to global warming. So far, most of the efforts in understanding the response of the tropical Pacific climate to global warming simulated by coupled GCMS have largely been concentrated on factors within the tropics (Knutson and Manabe 1995; Meehl and Washington 1996; Vecchi et al. 2006; DiNezio et al. 2009). The present study suggests that a tropical perspective alone may not be adequate in understanding the effects of global warming on the level of ENSO activity or on the mean state, particularly considering that the changes in the mean tropical upper-ocean stratification already include the response of ENSO to extratropical forcing.

Acknowledgments. The study is jointly supported by a grant from the National Basic Research Program of China (2007CB411806) and NSFC Grants (40675049 and 40821092). D.-Z. Sun was partially supported by the U.S. NSF's Climate and Large-Scale Dynamics Program and U.S. NSF's Physical Oceanography Program (ATM-9912434, ATM-0331760, and ATM 0553111). We are grateful to the editor Dr. Shangping Xie, and to the two anonymous reviewers, for their comments and suggestions.

REFERENCES

Bettge, T. W., J. W. Weatherly, W. M. Washington, D. Pollard, B. P. Briegleb, and W. G. Strand Jr., 1996: The CSM Sea Ice Model. NCAR Tech. Note NCAR/TN-425+STR, National Center for Atmospheric Research, Boulder, Colorado, 25 pp.

Bonan, G. B., K. W. Oleson, M. Vertenstein, S. Levis, X. Zeng, Y. Dai, R. E. Dickson, and Z.-L. Yang, 2002: The land surface climatology of the Community Land Model coupled to the NCAR Community Climate Model. *J. Climate,* **15,** 3123–3149.

Bradley, R. S., M. K. Hughes, and H. F. Diaz, 2003: Climate in medieval time. *Science,* **302,** 404–405.

Bush, A. B. G., and S. G. H. Philander, 1998: The role of ocean-atmosphere interactions in tropical cooling during the Last Glacial Maximum. *Science,* **279,** 1341–1344.

Cobb, K. M., C. D. Charles, H. Cheng, and R. L. Edwards, 2003: El Niño/Southern Oscillation and tropical Pacific climate during the last millennium. *Nature,* **424,** 271–276.

Collins, W. D., and Coauthors, 2003: Description of the NCAR Community Atmosphere Model (CAM2). NCAR Tech Note, 189 pp. [Available online at http://www.ccsm.ucar.edu/models/atm-cam/docs/cam2.0/description/index.html.]

Deser, C., M. A. Alexander, and M. S. Timlin, 1996: Upper-ocean thermal variations in the North Pacific during 1970–1991. *J. Climate,* **9,** 1840–1855.

DiNezio, P. N., A. C. Clement, G. A. Vecchi, B. J. Soden, B. P. Kirtman, and S.-K. Lee, 2009: Climate response of the equatorial Pacific to global warming. *J. Climate,* **22,** 4873–4892.

Fedorov, A., P. S. Dekens, M. McCarthy, A. C. Ravelo, P. B. deMenocal, M. Barreiro, R. C. Pacanowski, and S. G. H. Philander, 2006: The Pliocene paradox (mechanisms for a permanent El Niño). *Science,* **312,** 1485–1489.

Gu, D., and S. G. H. Philander, 1997: Interdecadal climate fluctuations that depend on exchanges between the tropics and extratropics. *Science,* **275,** 805–807, doi:10.1126/science.275.5301.805.

Jin, F.-F., 1996: Tropical ocean–atmosphere interaction, the Pacific cold tongue, and the El Niño–Southern Oscillation. *Science,* **274,** 76–78.

Knutson, T. R., and S. Manabe, 1995: Time-mean response over the tropical Pacific to increased CO_2 in a coupled ocean–atmosphere model. *J. Climate,* **8,** 2181–2199.

Liu, H. L., X. H. Zhang, W. Li, Y. Q. Yu, and R. C. Yu, 2004: An eddy-permitting oceanic general circulation model and its preliminary evaluations. *Adv. Atmos. Sci.,* **21,** 675–690.

Liu, Z., S. G. H. Philander, and P. C. Pacanowski, 1994: A GCM study of tropical–subtropical upper-ocean water exchange. *J. Phys. Oceanogr.,* **24,** 2606–2623.

McCreary, J. P., and P. Lu, 1994: On the interaction between the subtropical and the equatorial oceans: The subtropical cell. *J. Phys. Oceanogr.,* **24,** 466–497.

Mechoso, C. R., and Coauthors, 1995: The seasonal cycle over the tropical Pacific in coupled ocean–atmosphere general circulation models. *Mon. Wea. Rev.,* **123,** 2825–2838.

Meehl, G. A., and W. M. Washington, 1996: El Niño-like climate change in a model with increased atmospheric CO_2 concentrations. *Nature,* **382,** 56–60.

Neelin, J. D., D. S. Battisti, A. C. Hirst, F.-F. Jin, Y. Wakata, T. Yamagata, and S. Zebiak, 1998: ENSO theory. *J. Geophys. Res.,* **103,** 14 261–14 290.

Pedlosky, J., 1987: An inertial theory of the equatorial undercurrent. *J. Phys. Oceanogr.,* **17,** 1978–1985.

Rein, B., A. Lückge, L. Reinhardt, F. Sirocko, A. Wolf, and W.-C. Dullo, 2005: El Niño variability off Peru during the last 20,000 years. *Paleoceanography,* **20,** PA4003, doi:10.1029/2004PA001099.

Rodgers, K. B., P. Friederichs, and M. Latif, 2004: Tropical Pacific decadal variability and its relation to decadal modulations of ENSO. *J. Climate,* **17,** 3761–3774.

Schopf, P., and R. Burgman, 2006: A simple mechanism for ENSO residuals and asymmetry. *J. Climate,* **19,** 3167–3169.

Sun, D.-Z., 1997: El Niño: A coupled response to radiative heating? *Geophys. Res. Lett.,* **24,** 2031–2034.

——, 2000: Global climate change and ENSO: A theoretical framework. *El Niño: Historical and Paleoclimatic Aspects of the Southern Oscillation, Multiscale Variability and Global and Regional Impacts,* H. F. Diaz and V. Markgraf, Eds., Cambridge University Press, 443–463.

——, 2003: A possible effect of an increase in the warm-pool SST on the magnitude of El Niño warming. *J. Climate,* **16,** 185–205.

——, 2004: The control of meridional differential heating over the level of ENSO activity: A heat-pump hypothesis. *Earth's Climate: The Ocean–Atmosphere Interaction, Geophys. Monogr.,* Vol. 147, Amer. Geophys. Union, 71–83.

——, and T. Zhang, 2006: A regulatory effect of ENSO on the time-mean thermal stratification of the equatorial upper ocean. *Geophys. Res. Lett.,* **33,** L07710, doi:10.1029/2005GL025296.

——, ——, and S.-I. Shin, 2004: The effect of subtropical cooling on the amplitude of ENSO: A numerical study. *J. Climate,* **17,** 3786–3798.

——, and Coauthors, 2006: Radiative and dynamical feedbacks over the equatorial cold tongue: Results from nine atmospheric GCMs. *J. Climate,* **19,** 4059–4074.

Sun, F., and J.-Y. Yu, 2009: A 10–15-yr modulation cycle of ENSO intensity. *J. Climate,* **22,** 1718–1735.

Trenberth, K. E., G. W. Branstator, D. Karoly, A. Kumar, N.-C. Lau, and C. Ropelewski, 1998: Progress during TOGA in understanding and modeling global teleconnections associated with tropical sea surface temperatures. *J. Geophys. Res.,* **103,** 14 291–14 324.

van Oldenborgh, G. J., S. Y. Philip, and M. Collins, 2005: El Niño in a changing climate: A multi-model study. *Ocean Sci.,* **1,** 81–95.

Vecchi, G. A., B. J. Soden, A. T. Wittenberg, I. M. Held, A. Leetmaa, and M. J. Harrison, 2006: Weakening of tropical Pacific atmospheric circulation due to anthropogenic forcing. *Nature,* **441,** 73–76, doi:10.1038/nature04744.

Wang, B., H. Wan, Z. Z. Ji, X. H. Zhang, R. C. Yu, Y. Q. Yu, and H. L. Liu, 2004: Design of a new dynamical core for global atmospheric models based on some efficient numerical methods. *Sci. China,* **47** (Suppl.), 4–21.

Wang, C., and J. Picaut, 2004: Understanding ENSO physics—A review. *Earth's Climate: The Ocean–Atmosphere Interaction, Geophys. Monogr.,* Vol. 147, Amer. Geophys. Union, 21–48.

Xiao, C., and Y. Yu, 2006: Shape-preserving advection scheme and its application in an OGCM (in Chinese). *Prog. Nat. Sci.,* **16,** 1442–1448.

Yu, R. C., 1994: A two-step shape-preserving advection scheme. *Adv. Atmos. Sci.,* **11** (4), 479–490.

Yu, Y., and Coauthors, 2008: Coupled model simulations of climate changes in the 20th century and beyond. *Adv. Atmos. Sci.,* **25,** 641–654.

Zhang, X., G.-Y. Shi, H. Liu, and Y. Yu, 2003: The development and application of the oceanic general circulation models. Part I: The global oceanic general circulation models (in Chinese). *Chin. J. Atmos. Sci.,* **27,** 607–617.